Published in final edited form as:
Langmuir. 2010 November 16; 26(22): 17269–17277. doi:10.1021/la101791r.

Origin of the Nonadhesive Properties of Fibrinogen Matrices Probed by Force Spectroscopy

Ivan S. Yermolenko[‡,¶], **Alexander Fuhrmann**[†], **Sergei N. Magonov**[§], **Valeryi K. Lishko**[‡], **Stanislav P. Oshkadyerov**[¶], **Robert Ros**[†,*], and **Tatiana P. Ugarova**[‡,*]

[‡]Center for Metabolic Biology and School of Life Sciences

[†]Department of Physics, Arizona State University, Tempe, AZ 85287

[§]Agilent Technologies, Chandler, AZ 85224

[¶]Institute for Metal Physics, NAS of Ukraine, Kiev

Abstract

The deposition of a multilayered fibrinogen matrix on various surfaces results in a dramatic reduction of integrin-mediated cell adhesion and outside-in signaling in platelets and leukocytes. The conversion of a highly adhesive, low density fibrinogen substrate into the nonadhesive high density fibrinogen matrix occurs within a very narrow range of fibrinogen coating concentrations. The molecular events responsible for this transition are not well understood. Herein, single-cell and molecular force spectroscopy were used to determine the early steps in the formation of nonadhesive fibrinogen substrates. We show that adsorption of fibrinogen in the form of a molecular bilayer coincides with a several-fold reduction in the adhesion forces generated between the AFM tip and the substrate as well as between a cell and the substrate. Subsequent deposition of new layers at higher coating concentrations of fibrinogen results in a small additional decrease in adhesion forces. The poorly adhesive fibrinogen bilayer is more extensible under an applied tensile force than the surface-bound fibrinogen monolayer. Following chemical cross-linking, the stabilized bilayer displays the mechanical and adhesive properties characteristic of a more adhesive fibrinogen monolayer. We propose that a greater compliance of the biand multilayer fibrinogen matrices has its origin in the interaction between the molecules forming the adjacent layers. Understanding the mechanical properties of nonadhesive fibrinogen matrices should be of importance for therapeutic control of pathological thrombosis and in biomaterials science.

Introduction

The plasma protein fibrinogen plays a central role in normal hemostasis and wound healing. During blood vessel injury fibrinogen is converted into a fibrin clot, which seals the breach and prevents blood loss. Fibrinogen is a multifunctional protein and contains the binding sites for integrin adhesion receptors on platelets and leukocytes. Consequently, in addition to acting as the mechanical scaffold of clots, fibrin(ogen) can serve as an adhesive substrate for blood cells. While beneficial for the initial plug and fibrin clot formation, subsequent platelet adhesion must be strictly regulated to prevent their inappropriate accumulation. If

[*]To whom correspondence should be addressed: robert.ros@asu.edu and Tatiana.Ugarova@asu.edu.

Supporting Information Available: Kinetics of fibrinogen adsorption on mica, distribution of forces for the interaction of an unmodified AFM tip and a substrate prepared by adsorption of 0.6 μg/ml fibrinogen, dependence of adhesion forces observed between the AFM tip and adsorbed fibrinogen on substrate contact (dwell) time, and representative 2-D histograms generated from the force-distance curves obtained on surfaces prepared by adsorption of 5 and 20 μg/ml fibrinogen. This material is available free of charge via the Internet at http://pubs.acs.org.

not curtailed, uncontrollable platelet adhesion to fibrin can lead to their activation and thrombus propagation. Likewise, adhesion of leukocytes, which are known to contain potent fibrinolytic enzymes, must be regulated to allow early hemostasis to proceed unchallenged until the growth and stability of the fibrin plug is established. Therefore, a proper balance between adhesive and anti-adhesive mechanisms operating at the surface of fibrin clots in the circulation may play important roles in the control of thrombus formation, stability and timely dissolution. In addition to its role in hemostasis, fibrinogen deposition on implanted biomaterials may affect their biocompatibility by promoting adhesion of platelets and leukocytes which, as generally believed, can trigger such unwanted processes as thrombosis and inflammation.

Despite the importance for hemostasis and biomaterials science, the mechanisms that control the adhesive properties of fibrin clots and biomaterials *in vivo* are poorly understood. While numerous *in vitro* studies have documented that the surface of fibrin clots is highly adhesive for platelets and leukocytes, observations *in vivo*[1-4] indicate that fibrin is poorly adhesive for these cells suggesting the existence of natural anti-adhesive mechanisms. Likewise, whereas fibrinogen adsorbed on various biomaterials in model experiments supports efficient adhesion of blood cells, implanted vascular prostheses prepared by a “preclotting method”, with a flow surface consisting of a layer of fibrin, are paradoxically hypothrombogenic[5,6]. The surfaces of hemostatic clots and implanted biomaterials in circulation are continuously exposed to soluble fibrinogen, which is present at a high concentration. It is well established that fibrinogen can form complexes with fibrin[7]. Moreover, although it is much less appreciated, fibrinogen can self-associate without thrombin activation forming aggregates[8]. Therefore, a layer of aggregated fibrinogen may influence the adhesive properties of blood-contact surfaces.

We and others have recently demonstrated that deposition of fibrinogen on fibrin clots or its adsorption on various surfaces at increasing densities dramatically reduces adhesion of leukocytes and platelets[9-11]. Initial insights into the mechanism by which fibrinogen renders the surfaces nonadhesive, provided by studies using atomic force microscopy and force spectroscopy, have demonstrated that fibrinogen deposition at a high density results in an aggregated multilayered material characterized by low adhesion forces[10]. In contrast, adsorption of fibrinogen at a low density produces a single layer in which molecules are directly attached to the hard surface resulting in high adhesion forces. Consistent with their distinct physical properties, low, but not high density, fibrinogen induces strong integrin-mediated outside-in signaling in platelets, resulting in their spreading. These data suggest that deposition of a multilayered fibrinogen matrix decreases stable cell adhesion by modifying the physical properties of surfaces, which results in reduced force generation and insufficient signaling. Although the relationship between multilayer fibrinogen and reduced force generation is clearly established, the mechanisms underlying the formation of the nonadhesive fibrinogen matrix and its properties remain unclear.

Since a sharp decline in cell adhesion and adhesion forces occurs in a very narrow range of fibrinogen coating concentrations[9,10], we have examined the course of events that result in the creation of the nondhesive substrate. We show that the formation of the fibrinogen bilayer, characterized by the increased extensibility, initiates a steep reduction in the adhesion forces.

Materials and Methods

Materials

Human fibrinogen depleted of fibronectin and plasminogen was obtained from Enzyme Research Laboratories (South Bend, IN). Fibrinogen was treated with iodoacetamide to

inactivate the residual Factor XIII and then dialyzed against phosphate buffered saline (PBS). The concentration of fibrinogen was determined by spectrophotometry at 280 nm using the extinction coefficient 1.51 at 1 mg/ml. Fibrinogen was labeled with ^{125}Iodine using IODO-GEN (Thermo Scientific Pierce Protein Research Products, Rockford, IL), dialyzed against PBS and stored at −20 °C. The monoclonal antibody (mAb) 44a that recognizes the α_M integrin subunit was purified from the conditioned media of the hybridoma cells using Protein A agarose.

Cells

Human embryonic kidney 293 cells (HEK 293) stably expressing leukocyte integrin $\alpha_M\beta_2$ (aka Mac-1) have been described previously12،13. The $\alpha_M\beta_2$-expressing HEK 293 cells (HEK-Mac-1) and their wild-type counterparts (HEK-WT) were maintained in RPMI-1640 medium containing 10% fetal bovine serum, 100 IU/ml penicillin and 100 μg/ml streptomycin. Before each experiment, cells were detached from the flasks using the cell dissociation buffer (Cellgro, Mediatech Inc., Manassas, Virginia), washed twice in Hank's Balanced Salt solution (HBSS) containing Ca^{2+} and Mg^{2+} and resuspended in HBSS + 0.1% BSA.

Surface Preparation

To determine the kinetics of fibrinogen adsorption, different concentrations of ^{125}I-labeled fibrinogen (0.25-3 μg/ml) in PBS were incubated with freshly cleaved mica squares (8 × 8 mm) for various times at 37 °C. Excess fibrinogen was removed by rinsing the mica with water, and the bound fibrinogen was determined in a γ counter. For each concentration, the surface of mica became saturated with fibrinogen after 3 h. The time dependence of fibrinogen adsorption on mica is provided as Supporting Information Figure S1. The samples for AFM were prepared by adsorption of different concentrations of fibrinogen (0.05-20 μg/ml) in PBS onto freshly cleaved mica for 3 h at 37 °C. The samples were rinsed with water and dried with argon gas.

Cantilever Surface Modification for Single-cell Force Spectroscopy

Tipless silicon nitride cantilevers (HYDRA, AppNano, Santa Clara, CA) were plasma-cleaned at 29.6W, 400 mTorr in O_2 gas using a plasma cleaner (PDC-001, Harrick Plasma, Ithaca, NY). Cantilevers were incubated in 2 mM APTES ((3-Aminopropyl) triethoxysilane) in chloroform solution. After 40 min at 22 °C, the cantilevers were rinsed with chloroform, followed by ethanol and Millipore quality water. Cantilevers were incubated in 1.25 mM Bis(sulfosuccinimidyl) suberate sodium salt (BS^3, Sigma) solution for 30 min and then placed into 0.5 mg/ml concanavalin A (Sigma) solution for 30 min at 22 °C. Cantilevers were then rinsed in PBS and stored in 1 M NaCl at 4 °C. Decoration of tips with concanavalin A enables the firm capture of cells, presumably through cell surface carbohydrates, and was previously reported to be many times stronger than other receptor/ligand interactions14.

Single-cell Force Spectroscopy

Force-distance measurements were performed in HBSS supplemented with 0.1% BSA at 22 °C using a MFP-3D AFM (Asylum Research, Santa Barbara, CA) operating in contact mode. Tipless cantilevers with nominal spring constants of 0.035 N/m were used for force measurements. The spring constants for each cantilever were measured using the MFP-3D's built in thermal method. Cells were pippeted into the custom-made AFM chamber and a single cell was instantly picked up from the glass surface by pressing on a cell with a cantilever using a contact force of 500-2000 pN for 5-30 sec. After that time, the cell was lifted from the surface, allowed to attach firmly to the cantilever for 5 min and then lowered

onto the fibrinogen substrate. The surfaces coated with different concentrations of fibrinogen were probed using a force trigger of 1 nN, approach and retract velocity of 2000 nm/s and dwell time on the surface from 0.01 to 150 sec. After the trigger force was reached, the z-position was kept constant. Since thermal drift during the dwell times can result in reduced contact force, the force acting on the cell during the dwell time was ≤ 1 nN. After each force measurement, a cell was allowed to recover for at least 2 min before the next cycle. For each contact time, 3-10 force measurements were performed. The dwell time dependent measurements were performed in a random order to ensure that adhesion properties of the cell during the pulling experiment remain unchanged. As monitored optically, the cells always detached from the fibrinogen substrate, but not from the cantilever during pulling. Cell detachment was indicated by the superimposition of trace and retrace baselines over pulling ranges (25-35 μm). The pulling speed of 2000 nm/s was chosen to reduce hydrodynamic drag effects on the cantilever15.

Atomic Force Microspcopy (AFM) Imaging of Fibrinogen

Images in air were acquired using an Agilent 5500 scanning probe microscope (Agilent Technologies, Chandler, AZ). Imaging was conducted in the amplitude modulation oscillatory mode using Si probes with stiffness in the 1-5 N/m range. The experimental parameters (small free amplitude in the 5-10 nm range and set-point amplitude close to free amplitude) were selected to perform a low-force operation, which prevents sample damage. The scan rate was 0.6-1.2 Hz. Images were analyzed to calculate the surface coverage by the fibrinogen molecules using Gwyddion 2.10 software.

Molecular Force Spectroscopy

Force-distance measurements of fibrinogen substrates were performed in PBS at room temperature using a MFP-3D AFM (Asylum Research, Santa Barbara, CA) operating in contact mode. Silicon nitride probes (MLCT, Veeco Probes, Camarillo, CA) with nominal spring constants in the range of 0.015-0.020 N/m were used for force measurements. The surfaces coated with different concentrations of fibrinogen were probed using a force trigger of 600 pN and an approach and retract velocity of 2000 nm/s. Force curves were collected using the built in “Force Map” procedure. With the scan size area of 1 × 1 μm, 64 × 64 arrays (15.625 nm per force curve) and a total amount of 4096 force-distance curves were collected for each surface measurement. A representative force map is shown as Figure S2 in the Supporting Information. Each curve was analyzed by a custom program written in IGOR Pro 6 (Wavemetrics, Lake Oswego, OR), which calculates adhesion (pull-off) forces. The most probable adhesion forces were obtained from the maximum of the Gaussian fit to the force histogram.

Data Analysis

To distinguish the two types of curves in the population of force-distance curves obtained on different fibrinogen surfaces in molecular force spectroscopy experiments, the following considerations have been used. The adhesion force between the sample and cantilever is defined as a pull-off force, which is the force difference between the base line and the point where the cantilever loses the contact with the surface. A requirement is that the surfaces are rigid but not deformable or elastic. This condition is met when fibrinogen is deposited at the low concentrations (0.05-0.8 μg/ml) and the molecules are attached directly to the mica surface. In this case, the adhesion part of the force-distance curve follows the same linear path as the positive contact part. At higher concentrations (>1-1.2 μg/ml), fibrinogen is deposited in the form of aggregated material which is not completely rigid. Under these circumstances, the adhesion part of the force-distance curve becomes nonlinear because the cantilever pulls aggregated fibrinogen from the surface. Unless there are clear rupture events, this part is still considered to be part of adhesion. In order to analyze the data

quantitatively, the force-distance curves in the adhesion part were fitted by a second degree polynomial essentially as described16. The data were collected using custom software which analyzes the force-distance curves in an automated manner. The distances (in nanometers) obtained from the raw force distance curves were defined as “length”, while those corrected for cantilever binding were denoted as “adhesion length”.

Results

Single-cell Force Spectroscopy (SCFS)

Using force spectroscopy with an unmodified AFM tip, we have previously shown that fibrinogen deposited on various surfaces at densities >2 μg/ml generates lower adhesion forces compared to the substrates prepared by deposition of lower (0.6-0.9 μg/ml) protein concentrations10. To examine whether cellular integrins detect the differences in the adhesive properties of fibrinogen substrates, SCFS experiments were performed. Single HEK-Mac-1 and HEK-WT cells were attached to a ConA-functionalized AFM cantilever, and then, each cell was brought into contact with the surfaces prepared by deposition of 0.6, 2 and 20 μg/ml of fibrinogen. Cells were pressed onto each matrix with a force of 1 nN for various times (<150 s). After each contact, the cantilever was withdrawn at a speed of 2000 nm/s. A schematic diagram of the SCFS experiment and a representative rupture pattern for the HEK-Mac-1 cell detached from freshly cleaved uncoated mica and mica coated with 0.6 μg/ml fibrinogen are shown in Figure 1. A typical retraction force curve displayed the maximum detachment force followed by several unbinding events of a smaller scale. This pattern was similar to that described previously for other integrin-ligand interactions17¯19. The maximal detachment force (F_{max}) was determined from the maximal cantilever deflection during retraction. Figure 2A shows that cell adhesion to the substrate prepared by adsorption of 0.6 μg/ml fibrinogen was contact time dependent and that between 10 and 120 s of substrate contact, the maximal forces required for cell detachment increased from 640 ± 110 pN to 1700 ± 200 pN. By contrast, cell adhesion to the substrate prepared by deposition of 2 and 20 μg/ml fibrinogen was characterized by low detachment forces (200-400 pN) at all tested contact times (Figure 2A, shown for 2 μg/ml). At 120 s, the maximal detachment force was ~6-fold higher on 0.6 μg/ml fibrinogen than that on 20 μg/ml (Figure 2B). To confirm that adhesion of HEK-Mac-1 cells was integrin-dependent, cells were preincubated with mAb 44a directed against the α_M subunit of Mac-1. As shown in Figure 2B, no significant cell adhesion to 0.6 μg/ml fibrinogen was observed in the presence of the mAb. In another specificity control, adhesion of HEK-WT cells to 0.6 μg/ml fibrinogen demonstrated small detachment forces (190 ± 60 pN) that were comparable with those obtained for cell adhesion in the presence of mAb 44a. In addition, detachment forces for cell adhesion to uncoated mica were small at all contact times (280 ± 60 pN). Thus, by two approaches, SCFS and using an unmodified AFM tip10, fibrinogen deposited at higher densities generated drastically reduced adhesion forces than that adsorbed at low concentrations.

Adhesion Forces of Fibrinogen Substrates Determined by Force Spectroscopy

Our previous study 10 has shown that adhesion forces between an unmodified AFM tip and the fibrinogen substrates are several-fold higher on 0.6 than on 2 μg/ml fibrinogen. Since the steep reduction in the adhesion forces occurs in a very narrow range of fibrinogen coating concentrations, we have analyzed this area in more detail. Accordingly, mica was coated with small increments of fibrinogen concentrations in the range between 0.6-2 μg/ml, and the adhesion forces of the surfaces were probed using AFM tip. Figure 3A and B show the most probable adhesion forces obtained from the Gaussian fits to the histograms versus the fibrinogen coating concentrations and the histograms of distribution of adhesion forces for selected concentrations of fibrinogen, respectively. The results confirmed that the surface-

AFM tip interaction was the strongest at the 0.6-0.7 μg/ml coating concentrations of fibrinogen (~210 pN) and showed that the increase from 0.7 to 1.5 μg/ml resulted in a ~ 2.7-fold decrease in the adhesion forces. The subsequent increase in the concentration of fibrinogen from 1.5 to 2 μg/ml and higher (up to 20 μg/ml) resulted only in an additional 1.25-fold decrease in adhesion forces. Thus, with increasing concentrations of adsorbed fibrinogen, a nonlinear dependence in adhesion forces was revealed; i.e., between 0.7 and 1.5 μg/ml there was a steep decline in the adhesion force (~160 $pN \cdot \mu g^{-1} \cdot ml$) whereas between 1.5 and 20 μg/ml adhesion forces decreased by ~0.5 $pN \cdot \mu g^{-1} \cdot ml$.

In a second set of studies, the dependence of the adhesion force on the time of the AFM tip-fibrinogen interaction was examined. Figure S3 in the Supporting Information shows that the increase in the tip dwell time from 0.02 to 0.5 s resulted in the augmentation of adhesion forces for each tested concentration of fibrinogen. However, the highest forces were still observed at the lowest density of the protein (0.7 μg/ml). Collectively, the data indicate that the largest drop in adhesion forces occurs in a very narrow range of the coating concentrations of fibrinogen.

The Thickness and Composition of Fibrinogen Matrices

Our previous visualization of fibrinogen by AFM showed that the surfaces prepared by deposition of 0.6-0.9 μg/ml fibrinogen consist of a single layer in which the individual molecules are easily discernible and immobilized on mica in the horizontal orientation 10. At higher coating concentrations (>1.2 μg/ml), the molecules began to pile up forming additional layers. Analyses of AFM images of fibrinogen adsorbed at 0.6 μg/ml demonstrated that the height of single molecules was 1.2 ± 0.2 nm (Figure 4A, *upper left image*). Furthermore, the height of the substrate deposited at 2 μg/ml determined by nanolithography was 2 ± 0.85 nm[10]. These data suggested that adsorption of fibrinogen in the range of nonadhesive concentrations (1.2-2 μg/ml) may result in its deposition in the form of ~ 2 molecular layers.

To investigate the composition of the nonadhesive fibrinogen substrates further, we analyzed the formation of the second fibrinogen layer using the AFM images. The height of the immobilized fibrinogen monolayer 1.2 ± 0.2 nm was selected to generate a mask (in the image processing program Gwyddion) that best approximates the height of the first fibrinogen layer. In the next step, the mask was applied to assess the presence of the second layer in the matrices prepared by adsorption of the higher concentrations of fibrinogen. The upper panels in Figure 4A show the images of selected fibrinogen surfaces. Below each image is the generated mask with only molecules in the second layer being visible. Adsorption of fibrinogen at 0.9 μg/ml resulted in only of few molecules seen on the top of the first layer. The number of molecules in the second layer increased at the higher concentrations of fibrinogen. Representative images of fibrinogen molecules in the second layer of matrices deposited at 1.2 and 1.5 μg/ml are shown in Figure 4B together with tracings of individual molecules and their domains. Figure 4C shows a schematic representation of the molecular packing in the first and second layers. Although some trinodular molecules are clearly seen in the second layer, there are also many globular structures, especially at 1.2 μg/ml. These evidently represent individual protein domains projecting from the first layer; however, their assignment within the fibrinogen structure and the mode of packing are problematic. Nevertheless, it appears that between 0.9 and 1.5 μg/ml, a portion of the molecules have their domains in the two layers simultaneously, i.e., some of fibrinogen domains are being attached directly to mica while others projected into the second layer.

The application of the mask allowed the calculation of a total area occupied by the first and second layers at each concentration. Figure 4D (squares) shows that the surface was

gradually covered by immobilized fibrinogen molecules in the first layer and became fully saturated at ≥ 1.4 μg/ml. The data also demonstrated that at 0.9 μg/ml, when the molecules in the first layer covered ~70% of the surface, the second layer began to form (~5% of the surface coverage). At 1.2 μg/ml, when the first layer occupied ~ 90% of the surface, the molecules in the second layer filled ~30% of a total area (Figure 4D, circles). Coinciding with the full mica coverage (at ≥1.4 μg/ml) was the deposition of the molecules in the second layer only, which reached a nearly complete surface coverage at 2 μg/ml. Taken together, the results suggest that in the range of coating concentrations between 0.9 and 1.5 μg/ml, when the fibrinogen matrix acquires its nonadhesive properties, the molecules begin to form a bilayer.

Two Types of Adhesion Curves Revealed by Analyses of Force-Distance Curves

Close examination of the force-distance curves in the force spectroscopy experiments above revealed two types of adhesion curves depending on the coating concentration of fibrinogen. These curves differ in the adhesion length, which is defined as the distance between the point where the cantilever starts bending toward the surface due to the attractive (adhesion) forces and the point where it loses contact with the surface during retraction. The two representative curves are shown in Figure 5A. Type 1 is characterized by a nearly linear relationship between the force and distance (denoted l_1) while Type 2 has a nonlinear concave shape and displays a higher adhesion length (denoted l_2) (Figure 5A, inset). Type 2 curves usually displayed several small unbinding events preceding the major rupture event. When plotted as the distribution of adhesion force data against the adhesion lengths for each fibrinogen concentration, the two-dimensional (2D) histograms revealed the presence of two types of surfaces characterized by different adhesion properties depending on the fibrinogen coating concentrations (Figure 5B). At 0.6 μg/ml, a 2D histogram demonstrated a single population of force-distance curves that are characterized by Type 1 adhesion lengths. As the coating concentration increased to 0.9 μg/ml, two populations of force-distance curves could be distinguished. Specifically, within a total population of the analyzed curves, Type 2 curves constituted 29% (n=436) of the adhesion cycles while those that belonged to Type 1 (n=937) represented 71%. The increase in the concentration of fibrinogen to 1.5 μg/ml resulted in the increase of Type 2 curves (44%) with a coincident decline of Type 1 curves (56%). At 2 μg/ml, Type 2 curves were predominant. At still higher fibrinogen densities (5 and 20 μg/ml), only a single population consisting of Type 2 curves was present (Figure S4 in the Supporting Information). Figure 5C shows the master curves with adhesion lengths corrected for cantilever bending constructed from a data set of single measurements as described16. In addition, the molecular extensions for Type 1 and Type 2 curves (corrected for cantilever bending) as well as the values of compliance (dl/dF) determined from force-extension curves at 50 pN applied force are presented in Table 1. It should be noted that the applied force in this case is a tensile force. The higher values of slopes, dl/dF, at a selected tensional force correspond to an increased deformability of the fibrinogen layer. The presence of Type 1 and 2 curves may reflect variations in the molecular composition/packing of the fibrinogen substrates. Indeed, the distribution of the two types of adhesion curves at 0.6, 0.9, 1.5 and 2 μg/ml correspond closely to the percentage of molecules in the first and second layers (Figure 4D). Furthermore, since Type 2 curves are characterized by higher adhesion lengths at any given force than Type 1 curves, the data suggest that the second layer is more extensible than the layer attached to mica.

To determine whether the higher extensibility of the second layer could be implicated in the lower adhesion forces, the fibrinogen molecules in the 1.5 μg/ml matrix were cross-linked with the bifunctional reagent Bis(sulfosuccinimidyl) suberate (BS^3). To achieve cross-linking, a monolayer was first formed by incubating the mica with 0.6 μg/ml fibrinogen, then the solution was aspirated and BS^3 was added. After 30 min, BS^3 was removed and

fibrinogen at 0.9 μg/ml was added. Sequential addition of the reagents was a prerequisite for the cross-linking of the molecules between the layers. As a control, N-hydroxysccinimidyl suberate (NHS), which represents a half of the BS^3 molecule, was substituted for BS^3. As shown in Figure 6, the control 1.5 μg/ml fibrinogen matrix produced by the addition of two fibrinogen solutions one after another displayed the distribution of adhesion curves similar to that in the matrix generated by deposition of 1.5 μg/ml fibrinogen during a single application (~1:1 ratio of Type 1 and Type 2 curves). A similar distribution was observed in the presence of NHS, suggesting that the cross-linker itself does not alter the fibrinogen structure. Also, no changes in the AFM topographical images after cross-linking were detected. Cross-linking of this matrix with BS^3 resulted in its conversion into a substrate characterized by an increased percentage of Type 1 curves (~85%). Moreover, the molecular extension and compliance of the Type 1 component of the cross-linked matrix (0.1±0.1 nm and 0.005±0.001 nm/pN) were similar to those of the 0.6 μg/ml fibrinogen monolayer and the surface-bound layer within the 1.5 μg/ml matrix (Table 1). Crosslinking also resulted in the increase of the most probable adhesion forces for Type 1 curves by ~1.4-fold. This increase corresponds to the difference in adhesion forces (~1.4-fold) exhibited by surface-bound layers (i.e., Type 1 curves) within the matrices prepared by adsorption of 0.6 and 1.5 μg/ml fibrinogen (Figure 5C). The 2D histograms of the cross-linked and control matrices, as well their characteristics, are shown in Figure S5 and Table S1 in the Supporting Information. The results indicate that linking the upper molecular layer to the underlying one (which, in turn, is attached to the mica) renders the matrix less extensible.

Discussion

In previous studies we established that a steep decline in integrin-mediated cell adhesion occurring in a very narrow range of fibrinogen coating concentrations correlated with the decrease in adhesion forces measured by AFM-based force spectroscopy10. In this study, we confirmed this observation using single cell force spectroscopy: i.e., adhesion forces developed between a cell and the substrate prepared by adsorption of 0.6 μg/ml fibrinogen were several-fold higher than those between a cell and fibrinogen deposited at 2 μg/ml. The results of the present study demonstrate that in this range of concentrations, fibrinogen is deposited in the form of a molecular bilayer which is sufficient to render the substrate incapable of sustaining high adhesion forces. Within this nonadhesive substrate, the majority of fibrinogen molecules in the lower layer are firmly attached to a hard surface and deposited in the side-on orientation while those in the upper layer are horizontally positioned above them. Deposition of the second layer produces a substrate which is more extensible under applied force than the surface-bound layer. Further increases in the number of fibrinogen layers result only in a small additional decrease in the adhesion forces. These findings indicate that a molecular bilayer is a minimal structural element of the nonadhesive fibrinogen substrate and suggest that the interaction between fibrinogen molecules in the layers results in the formation of a qualitatively new matrix incapable of supporting firm cell adhesion.

The conclusion that fibrinogen is deposited as a molecular bilayer is based upon the height of individual molecules determined from the AFM images as well as the thickness of the fibrinogen matrix measured by nanolithography. An average height of fibrinogen molecules attached to mica was assessed to be 1.2 ± 0.2 nm, which is in agreement with the data reported by Van De Keere20 for the D domains, but somewhat lower than the mean height of 1.7-2.4 nm reported by others21,22. Moreover, both numbers are significantly lower than those determined from the crystal structure of human fibrinogen (6.5 and 5 nm for the D and E domains, respectively) 23;24. The decrease in the height of adsorbed fibrinogen was previously explained by its time-dependent conformational spreading on surfaces22,25,26. A longer adsorption time in our experiments may explain why the height of the fibrinogen

molecules was lower than that of the protein adsorbed in other studies 21,22. Furthermore, there may be differences in spreading that result from dehydration of the molecule during the preparation of the AFM sample and its imaging. On the basis of our estimates from nanolithography, the height of a matrix prepared by adsorption of 2 μg/ml fibrinogen on mica was ~ 2 nm (10) which corresponds to two molecular layers. The numbers determined from AFM images and nanolitography are in a good agreement with an assessment of the surface topography using a mask which allows the dissection of the first and second fibrinogen layers (Figure 4).

Analyses of the force-extension curves acquired on fibrinogen matrices deposited as a mono- or bilayer revealed two different force extension characteristics. There was a clear transition from the matrices that produce a single type of curve with smaller lengths (at 0.6 μg/ml) to those that contain a mixed population of curves (at 1.5 μg/ml) and then to the substrates that display a uniform population of curves with longer lengths (at 2 μg/ml). The analyses indicate that for the applied forces in the range of 50-100 pN, the fibrinogen bilayer displays a substantial elongation whereas a monolayer shows virtually no elongation. For example, there is an 18-fold difference in the adhesion length between Type 1 and Type 2 curves for a force of 50 pN (Figure 5C and Table 1). The matrices prepared by adsorption of the higher concentrations of fibrinogen (>2 μg/ml) and in which the molecules are deposited as a multilayered material are even more extensible. However, the steepest increase in compliance still occurs when the substrate is converted from a monolayer into a bilayer. The characteristics of the monoand bi(multi)layer fibrinogen matrices suggest that these substrates have very different mechanical properties.

If the higher adhesion forces produced by the fibrinogen monolayer attached directly to a hard surface are relatively simple to understand, the origin of the low adhesion forces generated by the fibrinogen bilayer is unclear. When the AFM tip (or cellular integrin) pulls on the substrate, the molecules held by weak non-covalent bonds within a bilayer may locally separate from each other because the self-association of fibrinogen does not involve strong complimentary binding sites compared to those involved in fibrin polymerization. In this regard, AFM studies by Averett et al27 documented that the force required to rupture bonds between fibrin molecules was 191±21 pN, which is ~2.5 times the adhesion force required to detach the AFM tip from the fibrinogen bilayer in our studies. The finding that chemical cross-linking of the molecules within a bilayer reduces the extensibility of the substrate and increases adhesion forces suggests that the separation of the layers may be responsible for the decline in adhesion forces. It is also possible that the AFM tip (or a cell) may tear away fibrinogen molecules weakly bound to the underlying fibrinogen layer. In this regard, we have previously demonstrated that the AFM tip may occasionally pick up the fibrinogen from the substrate10. This observation may hint that the transfer of fibrinogen to the tip, especially when the probe touches the high-density multilayered matrix, may contribute to the decrease in adhesion forces. However, the transfer of fibrinogen was not readily demonstrable in SCFC experiments. In fact, we observed reproducible force adhesion curves when the same cell was allowed to adhere several times to the substrates prepared from 2 and 20 μg/ml fibrinogen, suggesting that a transfer of fibrinogen from the substrate to the cell was not the major factor in reduced cell adhesion. Nevertheless, further studies are needed to determine whether cellular integrins can remove fibrinogen from the substrate, as well as the molecular nature of the bonds that are under tension in the extensible multilayered fibrinogen.

Previous studies have proposed that fibrinogen deposition on the surface may occur in two alternative orientations, horizontal (end-on) and vertical (side-on), at the low and high coating concentrations, respectively, with horizontal packing being defined as the molecule lying down parallel to the substrate surface and vertical packing as an orientation in which

elongated fibrinogen molecules stand perpendicular to the substrate surface11,28-31. Our previous10 and present data are consistent with studies21,22 that observed that at 0.5-1 μg/ml, the fibrinogen molecules that attach to the surface are horizontal in orientation. Furthermore, although not clearly resolved, the molecules in the second layer are deposited in the horizontal orientation. Consistent with this interpretation, the height of the bilayer (~2 nm) agrees well with deposition of the molecules in the second layer in the horizontal orientation. Should the molecules be deposited vertically, a height of the bilayer would be close to 46 nm (the length of fibrinogen). Based on these findings, we suggest that a widely accepted model in which fibrinogen can adopt the side-on or end-on orientations depending on its concentration which was inferred from biophysical studies28-30, reflects, in fact, the differences in deposition of fibrinogen as a mono- and multilayer, respectively.

Fibrinogen adsorbed on mica at 5 and 20 μg/ml form thick deposits of ~5 and 9 nm, respectively, apparently consisting of several layers10. The mechanism by which fibrinogen is deposited as a multilayered material is unclear. Aggregation of fibrinogen on hard surfaces is phenotypically reminiscent of its self-assembly under certain experimental conditions8. However, whereas self-association of soluble fibrinogen in the presence of selected agents or under the conditions of high speed in the ultracentrifuge has been well documented, the fact that adsorption of fibrinogen on a surface triggers its aggregation is unappreciated. Immobilization of fibrinogen is known to elicit exposure of cryptic binding sites, including those for antibodies, integrins and other molecules32-37. Since following attachment to a surface fibrinogen begins to increase the molecular footprint in a manner that is consistent with its denaturation22,26,38, unfolding of the molecule may result in exposure of sequences involved in self-association. Indeed, we have previously demonstrated that denaturation of fibrinogen by urea rendered the protein competent to bind its soluble counterpart9. The deposition of fibrinogen in the second (and posterior) layer(s) should also result in the conformational changes and exposure of the self-association sites to account for the formation of the new layers. However, the extent of unfolding in the upper layers may be limited because the molecules attach to the soft underlying fibrinogen layers, but not to the hard mica surface. Regardless of the underlying mechanisms, the finding that fibrinogen forms a multilayer substrate on mica and glass10,39, in concert with previous data indicating that fibrinogen can aggregate on other surfaces40,41, suggests that the studies of fibrinogen adsorption as well as those of its interactions with purified integrins and cells may be markedly influenced by this process.

In summary, the present study supports and extends the concept that deposition of aggregated fibrinogen matrix decreases adhesion forces generated between the substrate and both the AFM tip and cellular integrins. The results suggest a model that the formation of the fibrinogen bilayer is a critical step in the dramatic reduction of adhesion forces. The proposed basis for reduced adhesion is an increased extensibility of the generated matrix arising from low forces that hold fibrinogen molecules within the matrix. Since fibrinogen is deposited on the surface of thrombi and implanted biomaterials, the mechanical properties of multilayer fibrinogen may play important roles in the responses of platelets and leukocytes during thrombus formation and in biomaterial applications.

Supplementary Material

Refer to Web version on PubMed Central for supplementary material.

Acknowledgments

This work was supported by the NIH grant (T.P.U.) and by start-up funds from Arizona State University (R.R.).

Reference List

1. Groves HM, Kinlough-Rathbone RL, Richardson M, Jorgensen L, Moore S. Lab. Invest. 1982; 46:605–612. [PubMed: 7087391]
2. van Ryn J, Lorenz M, Merk H, Buchanan M, Eisert WG. Thromb. Haemost. 2003; 90:1179–1186. [PubMed: 14652654]
3. van Aken PJ, Emeis JJ. Artery. 1982; 11:156–173. [PubMed: 7171326]
4. McGuiness CL, Humphries J, Waltham M, Burnand KG, Collins M, Smith A. Thromb. Haemost. 2001; 85:1018–1024. [PubMed: 11434678]
5. Yates SG, Barros D'Sa AA, Berger K, Fernandes LG, Wood SJ, Rittenhouse EA, Davis CC, Mansfield PB, Sauvage LR. Ann. Surgery. 1978; 188:611–622.
6. Patel M, Arnell RE, Sauvage LR, Wu HD, Shi Q, Wechezak AR, Mungin D, Walker M. Ann. Vasc. Surg. 1992; 6:244–251. [PubMed: 1535213]
7. Doolittle RF. Annu. Rev. Biochem. 1984; 53:195–229. [PubMed: 6383194]
8. Gollwitzer R, Bode W, Karges HE. Thromb. Res. 1983; (Supplement V):41–53. [PubMed: 6351336]
9. Lishko VK, Burke T, Ugarova TP. Blood. 2007; 109:1541–1549. [PubMed: 16849640]
10. Podolnikova NPYIS, Fuhrmann A, Lishko VK, Magonov S, Bowen B, Enderlein J, Podolnikov A, Ros R, Ugarova TP. Biochemistry. 2010; 49:68–77. [PubMed: 19929007]
11. Jirouskova M, Jaisawal JK, Coller BS. Blood. 2007; 109:5260–5269. [PubMed: 17332246]
12. Yakubenko VP, Lishko VK, Lam SCT, Ugarova TP. J. Biol. Chem. 2002; 277:48635–48642. [PubMed: 12377763]
13. Lishko VK, Yakubenko VP, Ugarova TP. Exp. Cell Res. 2003; 283:116–126. [PubMed: 12565824]
14. Wojcikiewicz EP, Zhang X, Moy VT. Biol. Proced .Online. 2010; 6:1–9. [PubMed: 14737221]
15. Janiviak H, Strukmeier J, Muller DJ. Eur. Biophys. J. 2005; 34:91–96. [PubMed: 15257425]
16. Fuhrmann A, Anselmetti D, Ros R, Getfert S, Reimann P. Physical Review. 2008; E 77(031912): 1–10.
17. Puech P-H, Taubenberger A, Ulrich F, Krieg M, Muller DJ, Heisenberg C-P. J. Cell Science. 2009; 118:4199–4206. [PubMed: 16155253]
18. Wojcikiewicz EP, Abdulreda MH, Zhang X, Moy VT. Biomacromolecules. 2006; 7:3188–3195. [PubMed: 17096550]
19. Taubenberger A, Cisneros DA, Friedrichs J, Puech P-H, Muller D, Franz CM. Mol. Biol. Cell. 2007; 18:1634–1644. [PubMed: 17314408]
20. Van De Keere I, Willaert R, Hubin A, Vereecken J. Langmuir. 2008; 24:1844–1852. [PubMed: 18193901]
21. Sit SP, Marchant RE. Thromb. Haemost. 1999; 82:1053–1060. [PubMed: 10494763]
22. Agnihotri A, Siedlecki CA. Langmuir. 2004; 20:8846–8852. [PubMed: 15379516]
23. Hall CE, Slayter HS. J. Biophys. Biochem.Cytol. 1959; 5:11–17. [PubMed: 13630928]
24. Weisel JW, Stauffacher CV, Bullitt E, Cohen C. Science. 1985; 230:1388–1391. [PubMed: 4071058]
25. Dahint R, Ros Seigel R, Harder P, Grunze M, Josse F. Sensors and Actuators B: Chemical. 1996; 35-36:497–505.
26. Wertz CF, Santore MM. Langmuir. 2002; 18:706–715.
27. Averett LE, Geer CB, Fuierer RR, Akhremichev BB, Gorkun OV, Schoenfisch MH. Langmuir. 2008; 24:4979–4988. [PubMed: 18351791]
28. Schaaf P, Dejardin P, Johner A, Schmitt A. Langmuir. 1987; 3:1128–1131.
29. Schaaf P, Dejardin P, Schmitt A. Langmuir. 1987; 3:1131–1135.
30. Kim J, Somorjai GA. J. Am. Chem. Soc. 2003; 125:3150–3158. [PubMed: 12617683]
31. Dyr JE, Tichy I, Jirouskova M, Tobiska P, Slavik R, Homola J, et al. Sensors and Actuators B: Chemical. 1998; 51:268–272.

32. Schielen WJG, Voskuilen M, Tesser GI, Nieuwenhuizen W. Proc. Natl. Acad. Sci. USA. 1989; 86:8951–8954. [PubMed: 2813432]
33. Zamarron C, Ginsberg MH, Plow EF. Thromb. Haemost. 1990; 64:41–46. [PubMed: 1703332]
34. Zamarron C, Ginsberg MH, Plow EF. J. Biol. Chem. 1991; 266:16193–16199. [PubMed: 1714910]
35. Ugarova TP, Budzynski AZ, Shattil SJ, Ruggeri ZM, Ginsberg MH, Plow EF. J. Biol. Chem. 1993; 268:21080–21087. [PubMed: 7691805]
36. Makogonenko EM, Tsurupa G, Ingham K, Medved L. Biochemistry. 2002; 41:7907–7913. [PubMed: 12069579]
37. Lishko VK, Kudryk B, Yakubenko VP, Yee VC, Ugarova TP. Biochemistry. 2002; 41:12942–12951. [PubMed: 12390020]
38. Santore MM, Wertz CF. Langmuir. 2005; 21:10172–10178. [PubMed: 16229542]
39. Wei G, Reichert J, Bossert J, Jandt K. Biomacromolecules. 2008; 9:3258–3267. [PubMed: 18937403]
40. Cassiafesta P, Humphris ADL, Jandt KD, Miles MJ. Langmuir. 2000; 16:8167–8175.
41. Sivaraman B, Latour RA. Biomaterials. 2010; 31:832–839. [PubMed: 19850334]

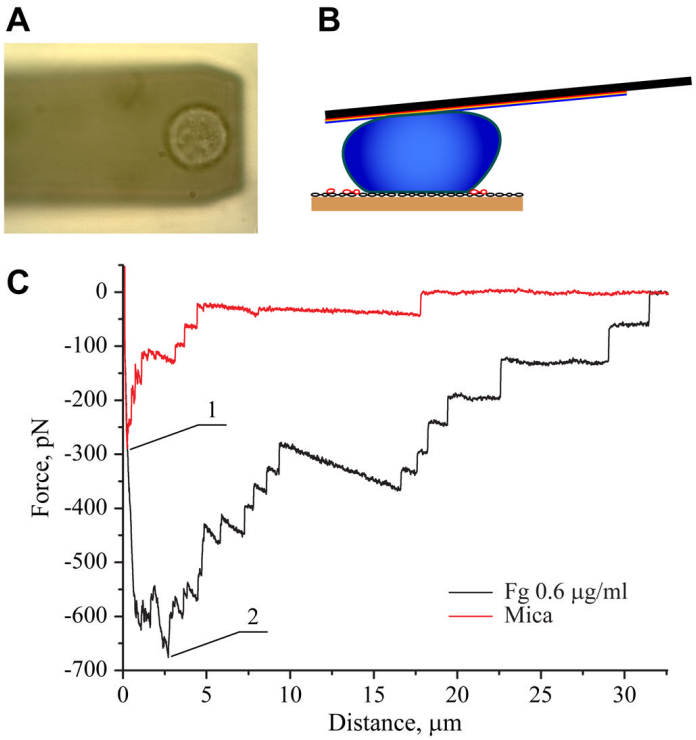

Figure 1.

Adhesion of the $\alpha_M\beta_2$-expressing cells to fibrinogen measured by SCFS. (A) An optical image of a living HEK-Mac-1 cell attached to the surface of the tipless cantilever. (B) Schematic representation of a cell attached to the cantilever during its contact with the adhesive fibrinogen substrate. (C) Representative force-distance curves for a HEK-Mac-1 cell brought in contact with fibrinogen coated on mica at 0.6 μg/ml (black curve) and, then, with a bare mica (red curve) for 10 s and pulled at 2 μm/s. Fg, fibrinogen. The numbers 1 and 2 indicate the maximal detachment forces for cell adhesion to the fibrinogen substrate and to mica, respectively.

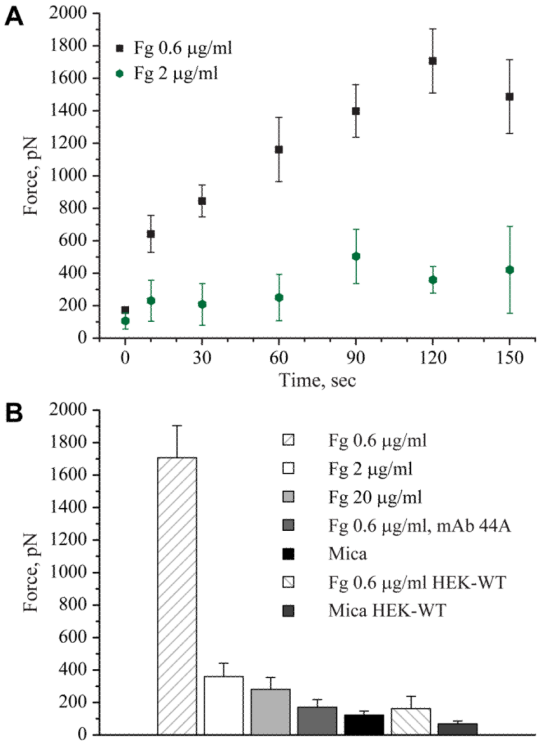

Figure 2.

Dependence of adhesion of the $\alpha_M\beta_2$-expressing cells on contact time with and the concentration of fibrinogen. (A) Mica was coated with 0.6 and 2 μ/ml fibrinogen and HEK-Mac-1 cell detachment forces were determined for contact times between 0 and 150 s. Adhesion of cells to fibrinogen substrates was measured by SCFS. The maximal detachment force (F_{max}) was determined from the maximal cantilever deflection during retraction. Detachment forces for cell adhesion to 0.6 μg/ml (19 cells; total 131 curves) and 2 μg/ml (5 cells; total 50 curves) are shown as the mean and standard deviation from 3-10 measurements performed with each cell. (B) Detachment forces determined for HEK-Mac-1 and HEK-WT cells adherent to different substrates for 120 s. In selected experiments, cells were preincubated for 20 min with anti-α_M mAb 44a (10 μg/ml) and their adhesion to 0.6 μg/ml fibrinogen was determined. Detachment forces for cells adherent to bare mica are also shown. Values represent the mean and standard deviation from 5-19 individual cells. Fg, fibrinogen.

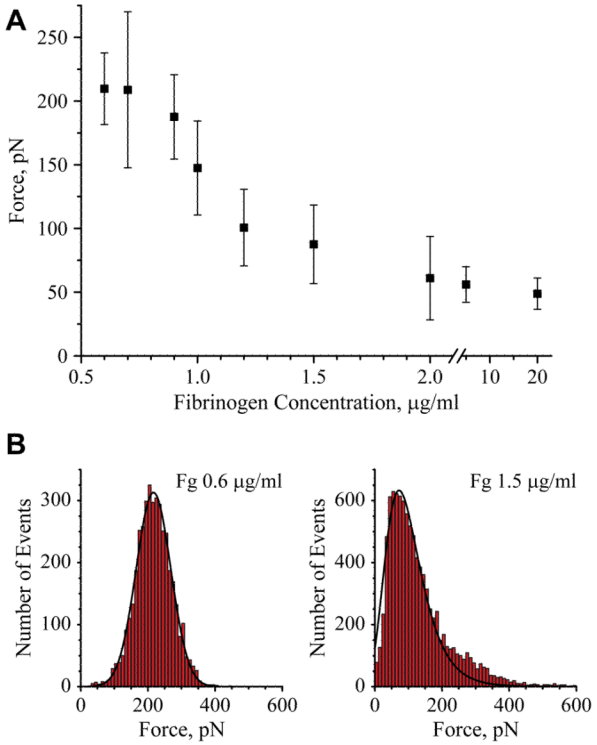

Figure 3.

Force spectroscopy analyses of fibrinogen substrates. (A) The most probable adhesion forces between an unmodified AFM tip and fibrinogen plotted as a function of the fibrinogen coating concentration adsorbed on mica. (B) Histograms with Gaussian fits of adhesion forces for selected (0.6 and 1.5 μg/ml) concentrations of fibrinogen deposited on mica. The data shown are means and standard deviation from 3-5 experiments with 20000-60000 force-distance curves collected from the force maps generated for each concentration of fibrinogen. The data for the substrate prepared by adsorption of 20 μg/ml fibrinogen were collected from 2 experiments in which 8000 force-distance curves were analyzed.

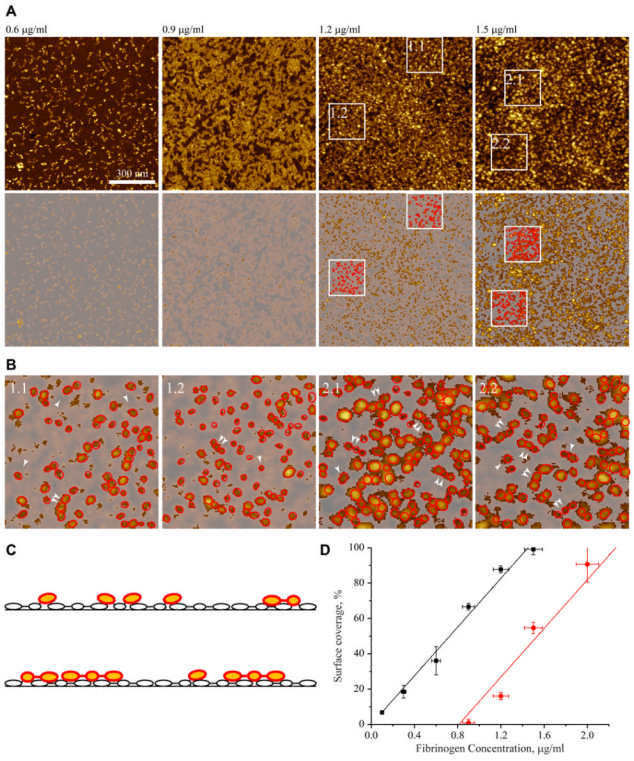

Figure 4.

Determination of the fibrinogen surface coverage. (A) AFM images of fibrinogen deposited at 0.6, 0.9, 1.2 and 1.5 μg/ml are shown in the upper row. After the application of the mask generated to cut off the molecules in the first layer, only the molecules in the second layer are seen (*bottom panels*). (B) Enlarged images of the material deposited in the second layer for surfaces prepared by adsorption of 1.2 μg/ml fibrinogen (fields 1.1 and 1.2) and 1.5 μg/ml (2.1 and 2.2) together with tracings of individual fibrinogen domains in red (single arrowheads). The selected trinodular fibrinogen molecules (46 nm) are indicated by double arrowheads. (C) A sketch drawn to show the orientation of the trinodular fibrinogen molecules in the first and second layers based on images in (B). The surface-bound molecules are shown as open ovals while those lying on the top of the first layer, are colored in yellow encircled with red. The molecules that are simultaneously attached to mica and protrude in the second layer are shown in two colors, with their surface-bound domains shown as open ovals and those that jut out in yellow/red. (D) The surface area covered by fibrinogen in the first (squares) and second (circles) layers was determined by the application of a mask with a cut-off at the mica surface or the first layer, respectively. Images were analyzed using Gwyddion 2.10 software. Since the increase in surface coverage did not result in the formation of compact ordered structures in the adsorbed layer, the overestimation of the molecular coverage due to the tip convolution does not change the character of the dependence of covered area on the coating concentration of fibrinogen. The data are expressed as a percentage of the total surface covered by fibrinogen deposited at each concentration. Vertical error bars represent S.D. of means of 2-6 images from 2 separate experiments, and horizontal error bars is S.D. for each input concentration of fibrinogen estimated as a pipette volume variability.

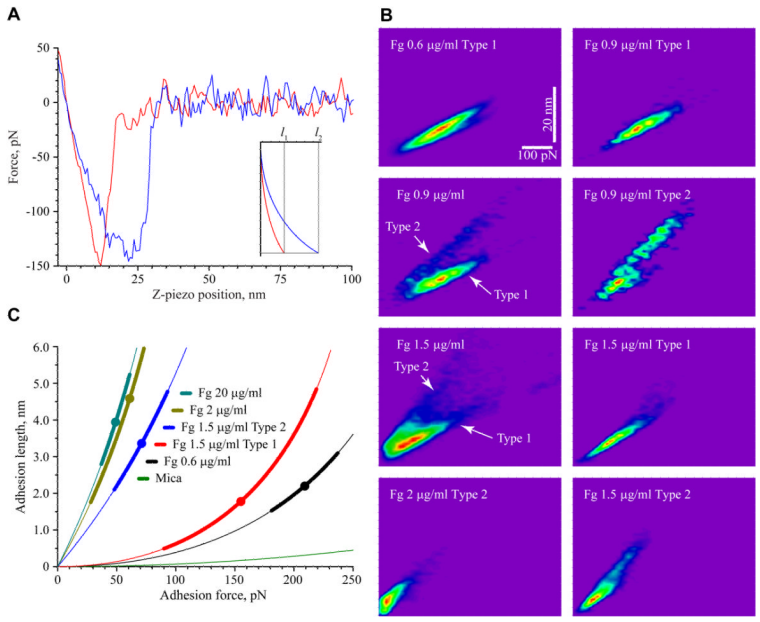

Figure 5.

Analyses of the force-distance curves produced by fibrinogen substrates. (A) Retracting parts of representative force-distance curves obtained on mica coated with 1.5 μg/ml fibrinogen. Inset shows representative master curves corresponding to the force-distance curves shown on the left constructed, as described16. The adhesion forces for the curves shown are ~145 pN (red) and ~150 pN (blue). The abscissa is a relative z-piezo position. (B) Adhesion force data for the substrates prepared by adsorption of 0.6, 0.9, 1.5 and 2 μg/ml fibrinogen are plotted against the length (from original force distance curves) in the 2D histograms. The data shown in the 2D histograms were interpolated using the bilinear interpolation function “Imageinterpolate” of IGOR Pro 6. The color code is “Rainbow” (red, high frequency; blue, low frequency; purple is the background). Fg, fibrinogen. (C) Master curves with adhesion lengths corrected for cantilever bending were constructed using the experimental data sets shown in *B*. The force-distance curves of single measurements (fitted by second degree polynomials) were accepted by the developed filtering procedure16 and used for the construction of master curves. The filled circle in each curve corresponds to a mean for the distribution in the force histograms and the thick lines correspond to standard deviation of the mean.

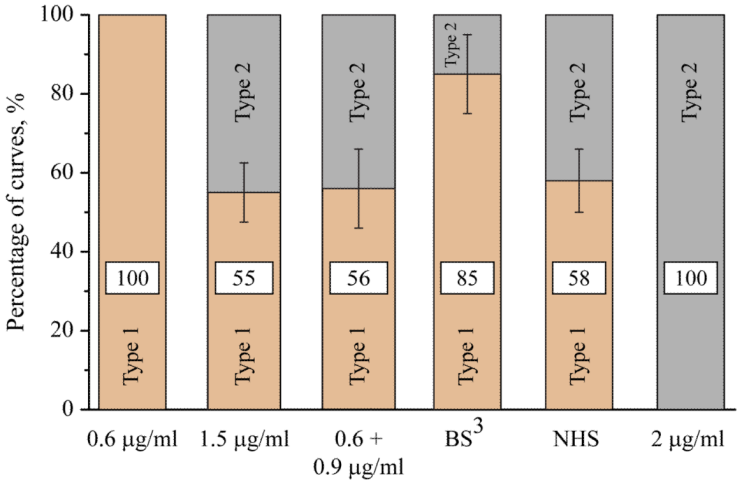

Figure 6.

Changes in the adhesive properties of the fibrinogen bilayer after its chemical cross-linking. A control fibrinogen monolayer prepared by adsorption 0.6 μg/ml exhibited only Type 1 of force-extension curves. The substrate prepared by adsorption of 1.5 μg/ml fibrinogen during a single application (denoted 1.5 μg/ml), and the substrate produced by coating mica first with 0.6 μg/ml fibrinogen for 1.5 h followed by the addition of 0.9 μg/ml fibrinogen for 1.5 h (denoted 0.9+0.6 μg/ml) exhibited a similar ~1:1 ratio of two types of the force-extension curves. BS^3 denotes the experiment in which the BS^3 cross-linker dissolved in PBS was added to the first layer prepared by adsorption 0.6 μg/ml fibrinogen. After 30 min, BS^3 was aspirated and 0.9 μg/ml fibrinogen was added for an additional 1.5 h. NHS denotes the experimental condition in which NHS was added after deposition of the first fibrinogen layer (0.6 μg/ml) followed by the addition of NHS and then 0.9 μg/ml fibrinogen. Similar to a control 1.5 μg/ml fibrinogen matrix, the generated substrate exhibited two types of curves. The bilayer prepared by deposition of 2 μg/ml fibrinogen displayed 100% of the Type 2 curves. The numbers within each bar indicate the percentage of Type 1 (light brown) or Type 2 (gray) force-extension curves.

Table 1

Molecular extensions (*l*) and compliance (d*l*/d*F*) of the fibrinogen matrices determined from force-extension curves at 50 pN applied tensile force.

Fibrinogen concentration, μg/ml	***l*, nm**	**d*l*/d*F*, nm/pN**
0.6	0.1±0.1	0.004±0.001
1.5 type 1	0.1±0.1	0.006±0.002
1.5 type 2	1.8±0.6	0.051±0.005
2	3.5±0.7	0.091±0.018
20	4.0±0.5	0.102±0.017